# Osmium Atoms and Os$_2$ Molecules Move Faster on Selenium-Doped Compared to Sulfur-Doped Boronic Graphenic Surfaces

Nicolas P. E. Barry,*[,†] Anaïs Pitto-Barry,[†] Johanna Tran,[†] Simon E. F. Spencer,[‡] Adam M. Johansen,[‡] Ana M. Sanchez,[§] Andrew P. Dove,[†] Rachel K. O'Reilly,[†] Robert J. Deeth,[†] Richard Beanland,[§] and Peter J. Sadler*[,†]

[†]Department of Chemistry, [‡]Department of Statistics, and [§]Department of Physics, University of Warwick, Gibbet Hill Road, Coventry CV4 7AL, United Kingdom

S *Supporting Information*

ABSTRACT: We deposited Os atoms on S- and Se-doped boronic graphenic surfaces by electron bombardment of micelles containing 16e complexes [Os(p-cymene)(1,2-dicarba-*closo*-dodecaborane-1,2-diselenate/dithiolate)] encapsulated in a triblock copolymer. The surfaces were characterized by energy-dispersive X-ray (EDX) analysis and electron energy loss spectroscopy of energy filtered TEM (EFTEM). Os atoms moved *ca.* 26× faster on the B/Se surface compared to the B/S surface (233 ± 34 pm·s^{-1} *versus* 8.9 ± 1.9 pm·s^{-1}). Os atoms formed dimers with an average Os–Os distance of 0.284 ± 0.077 nm on the B/Se surface and 0.243 ± 0.059 nm on B/S, close to that in metallic Os. The Os$_2$ molecules moved 0.83× and 0.65× more slowly than single Os atoms on B/S and B/Se surfaces, respectively, and again markedly faster (*ca.* 20×) on the B/Se surface (151 ± 45 pm·s^{-1} versus 7.4 ± 2.8 pm·s^{-1}). Os atom motion did not follow Brownian motion and appears to involve anchoring sites, probably S and Se atoms. The ability to control the atomic motion of metal atoms and molecules on surfaces has potential for exploitation in nanodevices of the future.
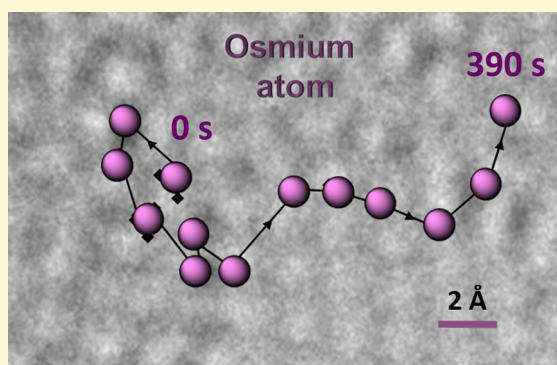
INTRODUCTION

There is a long history of using electron microscopes to image the motion of adatoms on a thin film,[1,2] but only recent advances have made it feasible to study the chemistry of metals at the level of atomic resolution.[3−7] In particular the thickness and regularity of the honeycomb network of graphene provides an exceptional support for the deposition of individual atoms and observation of their motion.[8] However, imaging the dynamics of single atoms on graphenic materials, compared to biomacromolecules and small clusters,[9,10] is technically difficult because of their subnanometric size and their fast motion.[11] Studies of the movement of Mo and W atoms on graphene and their trapping by defective sites have been reported,[12,13] as well as Pd and Te atoms which bind to the free edge states along graphene hole edges,[14] although much of our current knowledge of such migratory behavior of single atoms relies on theoretical elucidation.[15−19]

Recently we showed that electron beam irradiation of self-spreading polymer-encapsulated precious metal complexes can generate *in situ*-doped graphenic surfaces on which the dynamics of single metal atoms can be studied in real time using an aberration-corrected high resolution electron microscope.[28] Here we synthesize novel boron−sulfur-doped and boron−selenium-doped graphenic surfaces and study the atomic trajectories and rate of migration of single osmium atoms and individual Os$_2$ molecules. These experiments reveal the dramatic effect of two chalcogenide (group 16) dopants S and Se on osmium atom migration.

METHODS

The preparations of the complex [Os(p-cym)(1,2-dicarba-*closo*-dodecaborane-1,2-dithiolate)] (**1**) and of micelles **OsMs-S** were based on our previous reports.[20,28] Complex [Os(p-cym)(1,2-dicarba-*closo*-dodecaborane-1,2-diselenate)] (**2**) was synthesized following the same procedure as for complex **1** and characterized by elemental analysis (calcd (%) for [C$_{12}$H$_{24}$B$_{10}$OsSe$_2$]: C, 23.08; H, 3.87. Found: C, 23.35; H, 3.84). The triblock copolymer P123 [poly(ethylene glycol)-*block*-poly(propylene glycol)-*block*-poly(ethylene glycol)] was purchased from Sigma-Aldrich and used as received. Anhydrous tetrahydrofuran (Aldrich) was used. Deionized water (18.2 MΩ·cm purity) was collected from a Purelab UHQ USF Elga system. Lacy carbon grids were purchased from Elektron Technology U.K., Ltd., and used as received. Complex **2** was synthesized following the same procedure as for complex **1**. The synthesis of micelles **OsMs-Se** was carried out as follows. A tetrahydrofuran (THF) solution (1 mL) of complex **2** (5 mg/mL) was added to an aqueous solution (10 mL) of polymer P123 (5 mg/mL), and the resultant mixture was stirred at ambient temperature for 4 h. The solution was dialyzed to remove the THF (MWCO = 1000 Da), for 48 h, and then freeze-dried. The size of the **OsMs-Se** micelles
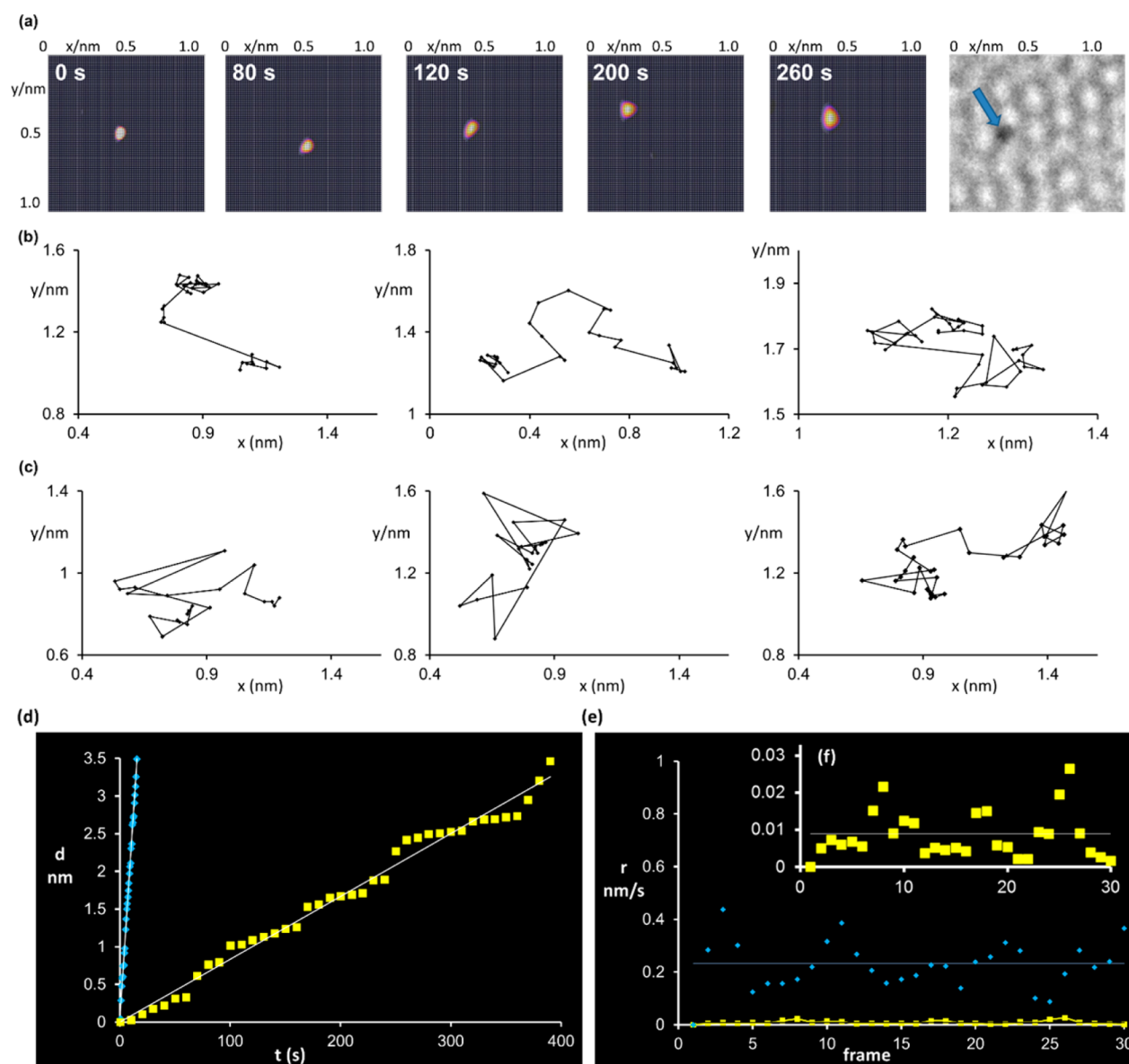
Figure 1. Positions, trajectory, and experimental hopping of an Os atom on the B/S- and B/Se-doped graphenic surfaces. (a) Example of experimental TEM images and the trajectory of an individual Os atom on the B/S surface recorded at different irradiation times (five frames extracted from a total of 40 pictures over a total irradiation time of 390 s). (b and c) Illustrative trajectories of three individual osmium atoms on the B/S- and B/Se-doped graphenic surfaces, respectively. Owing to the high contrast of osmium atoms as compared to the graphenic surfaces, the extraction of the coordinates of the atom in each frame is readily achieved from a 3D surface projection for each TEM picture (a). (d) Cumulative apparent distances covered by an individual Os atom on B/S (yellow) and B/Se (blue) surfaces. (e) Apparent speed of motion of an individual Os atom on B/S (yellow) and B/Se (blue) surfaces between each frame ($t = 0$ for first frame of each stack). (f) Enlargement of the B/S (yellow) plot shown in (e).

was found, by dynamic light scattering (DLS), to be 20.1 ± 0.5 nm, similar to the size of the analogous **OsMs-S** micelles.

High-Resolution Electron Microscopy (HR-TEM). A JEOL JEM-ARM200F HR-TEM was operated at 80 keV, 1.9 pA/cm², with spherical aberration (C_s) tuned to approximately +1 μm, and images were recorded on a Gatan SC1000 Orius CCD camera. All the images were analyzed with ImageJ (Fiji) software. All the stacks were aligned with the plugin software StackReg[21] before extracting the coordinates of the atoms. The image sequences were independently aligned using a Digital Micrograph script. Adjacent images were aligned by analysis of the normalized cross-correlation of a user-selected region in the image stack. The center of the cross-correlation peak was found to sub-pixel accuracy using either (a) the centroid of the correlation peak or (b) the fitting of parabolas to the peak in the x- and y-directions, while linear interpolation was used to produce sub-pixel image shift.

Computational Details. Density functional theory (DFT) geometry optimizations were carried out using the ORCA package,[22] version 3.0.1. The split-valence def2-SVP basis set[23] was used for all nontransition elements with the corresponding effective core potential basis set for Os.[24,25] The Perdew−Burke−Ernzerhof (PBE) functional[26] was employed including the resolution of identity approximation in an unrestricted framework for paramagnetic species. Grimme's D3(BJ) correction for dispersion[27] was also used throughout. To help improve SCF convergence, the default damping factor (DampFac) was increased from the default value of 0.7 to 0.9−0.98 depending on the behavior of the system in question.

■ RESULTS AND DISCUSSION

We synthesized two graphenic surfaces (Supporting Information Figure S1 for a low magnification image of the B/S surface). The

first was doped with heteroatoms boron and sulfur (B/S) following the procedure we described recently,[28] while the second was doped with heteroatoms boron and selenium (B/Se). This involved irradiating **OsMs-Se** micelles made of [Os(*p*-cymene)(1,2-dicarba-*closo*-dodecarborane-1,2-diselenate)] encapsulated in the triblock copolymer P123 with the electron beam of an aberration-corrected high resolution HR-TEM-STEM with a Schottky thermal field-emission source (80 keV; 1.9 pA cm^{-2} or 7.6 × 10^7 electrons nm^{-2} s^{-1}). In general there were regions of the surface which were single-layer (fast Fourier transform in Supporting Information Figure S1) and on which an idealized hexagonal lattice could be readily overlaid, although the surface was clearly inhomogeneous in some regions as expected from the presence of the B/S and B/Se dopants. The presence of boron and chalcogen atoms as well as osmium was confirmed by a combination of energy-dispersive X-ray (EDX) analysis and electron energy loss spectroscopy of energy filtered TEM (EFTEM) (Supporting Information Figure S2).

We investigated single Os atom migration by following the positions of individual Os atoms on B/S (over 390 s; 40 frames with 10 s between each frame) and B/Se surfaces (over 15 s; 31 frames with 0.5 s between each frame). The positions of each atom were extracted from a series of images from three different areas of the TEM grid. Successive images were aligned, and the drift was compensated by using the Plugin StackReg in Fiji-ImageJ[29] and by using a Digital Micrograph(TM) script (Methods section). Some sections of the surface are clearly hexagonal and of graphitic nature, whereas other areas are highly distorted by the dopants. Moreover, the atoms in the surface also undergo motion by absorption of energy from the beam. Nevertheless a consistent interpretation of Os atom movement can be obtained.

Density functional theory (DFT) calculations have predicted[19] that the presence of an Os atom adsorbed on a graphene matrix disturbs the structure of graphene when located at bridge- and edge-sites. This also appears to be the case with the multidoped graphenic surfaces. Supporting Information videos (Figures S3_Video 1 and S4_Video 2) show two examples of time-lapse TEM images used to extract the coordinates of the individual atoms on both B/S and B/Se surfaces. Perhaps surprisingly, since the surface is doped and not homogeneous graphene, it was possible to correlate the atom trajectories with the individual positions of the atom on idealized hexagonal grids as shown in Supporting Information Figures S5_Video 3 for the B/S matrix and S6_Video 4 for the B/Se matrix.

The experimental images highlight the existence of anchoring points on both surfaces, positions of apparent long residence times (Figures 1b,c). The analysis of the various trajectories suggests that the chalcogen atoms themselves induce the differences in atomic migration and have a direct impact on the trajectory of osmium atoms on the surface. This might involve direct Os–chalcogen binding, but the effects could also be propagated over a longer distance on the conjugated graphenic lattice. Supporting Information Figure S7 shows the trajectory of an individual Os atom on the B/S graphenic surface (Supporting Information Figure S7a), the superimposition of the atomic position on an ideal hexagonal monolayer graphene grid (Supporting Information Figure S7b), the apparent trapping sites (in blue in Supporting Information Figure S7c), and sites from which longer jumps than the average jump size are observed ("acceleration sites" in red in Supporting Information Figure S7c). From these data, three hypothetical chemical structures of the doped graphenic surfaces used in this study can be proposed

(Supporting Information Figures S7d–f): either the trapping sites are occupied by sulfur atoms and the accelerating sites are boron atoms (Supporting Information Figure S7d) or the opposite (Supporting Information Figure S7e); alternatively carbon atoms could act as acceleration sites, sulfur atoms act as trapping sites, and all the other sites where the osmium atom is seen moving to and from are occupied by boron atoms (Supporting Information Figure S7f). These three models are hypothetical since it is technically not possible to investigate the actual atomic composition of the surface site-by-site.

Interestingly, Cretu et al. have reported that W atoms are mobile on a graphitic surface but are trapped by defective sites.[13] They showed that below 250 °C, when the graphene lattice was heavily damaged by the beam, almost no jumps occurred and the W atoms were pinned by larger irradiation-induced lattice defects. In the range 250−500 °C, jumping of W atoms was observable, and escape from a trapping center could be induced thermally or by electron irradiation, a combination of thermal and beam effects which explains the observed small oscillations. In related work the same group observed the trapping of Mo atoms at defect sites in carbon nanotubes and in graphene,[12] and recently Pb and Te atoms have been trapped on amorphous graphene and at edge sites of holes in graphene.[14] Our experimental data are consistent with these previous observations and also show that such an escape by Os atoms from anchoring sites, at a temperature close to ambient, is dependent on the nature of the graphenic dopants.

We determined the apparent rate of migration of individual Os atoms on the two multidoped graphenic surfaces (average from observation of 10 single atoms). It should be noted that the real speed of motion of the atoms is at least the apparent monitored rate of migration, since we are limited by the speed of the camera and there could be more steps at intermediate times between frame captures. Figure 1d shows the dependence of the cumulative path length covered by two individual Os atoms (blue: B/Se surface; yellow: B/S surface) on irradiation time on the two surfaces. Remarkably, the chalcogen dopant (S *vs.* Se) dramatically influences the apparent rate of migration. The Os atom travels an apparent distance of 3.5 nm in 15 s on the B/Se surface, while the same distance is covered by the Os atom in 390 s on the B/S surface. This *ca.* 26× higher speed of Os atoms on the B/Se surface compared to the B/S surface (233 ± 34 pm s^{-1} versus 8.9 ± 1.9 pm s^{-1}, Supporting Information Table S1) is illustrated in Figure 1e and in Supporting Information Figure S8_Video 5. On both surfaces, the apparent rate of migration is not constant but varies over time, with significant autocorrelation (Figures 1e,f). This confirms the existence of anchors and suggests that the atom must receive a minimum energy from the high-energy electron beam to move from one anchoring site to another adjacent position. We found that an individual Os atom required irradiation for 70 ± 9 s on the B/S surface before hopping to another site, whereas on the B/Se surface, only *ca.* 1.5 ± 0.3 s of irradiation was required.

We also investigated the dynamics of migration of two close Os atoms on the B/S and B/Se surfaces. We elucidated the trajectory of each atom (Figure 2a) and thus the trajectory of the pair (Figure 2b,c). The atomic positions were extracted from a series of time-lapse TEM images, as for individual atoms. Supporting Information Figures S9_Video 6 and S10_Video 7 show examples for B/Se and B/S surfaces, respectively. Notably, the average Os–Os distances of 0.284 ± 0.077 nm on the B/Se surface and 0.243 ± 0.059 nm on B/S are both close to the Os–Os distance in metallic Os (0.27048 nm as the nearest neighbor
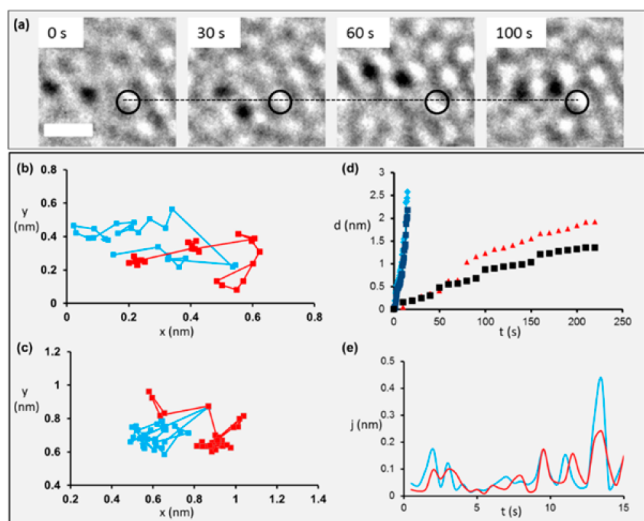
Figure 2. Positions, trajectory, and experimental hopping of Os_2 molecules on the B/S- and B/Se-doped graphenic surfaces. (a) HRTEM images showing the position of the two Os atoms on the B/S surface at different irradiation times (time = 0 s corresponding to the first image of the stack; scale bar = 0.5 nm). The black circles and the black dotted line show the alignment of the surface. (b) Trajectory of the hopping of the two Os atoms on the B/S surface over 390 s. (c) Trajectory of the hopping of the two Os atoms on the B/Se surface over 15 s. (d) Distances covered by each Os atom of a diatomic molecule on B/S (black and red) and B/Se (light and deep blue) surfaces. (e) Jump size against time for each atom of the molecule on the B/Se surface.

distance at 20 °C)[30] suggesting that these two Os atoms form a true Os_2 diatomic molecule. Furthermore, the two close Os atoms undergo concerted migration on the multidoped graphenic surfaces. The dependence of the jumping pattern for each Os atom shown in Figure 2c on irradiation time is shown in Figure 2e and confirms that the two atoms are indeed bonded.

Similar to the movement of isolated individual Os atoms, the distance traveled by each atom of the Os_2 molecule increases linearly with irradiation time on both surfaces (Figure 2d, Supporting Information Figure S9_Video 6, Figure S10_Video 7). The average apparent rate of migration of an Os_2 diatomic molecule on the B/S and B/Se surfaces (7.4 ± 2.8 pm s^{-1}, and 151 ± 45 pm s^{-1}, respectively, Supporting Information Table S1) was slightly slower (0.83× and 0.65×) than for individual Os atoms. Again, as for single Os atoms, the apparent rate of migration of Os_2 on the B/Se-doped surface was dramatically faster (ca. 20×) than on the B/S-doped surface (Supporting Information Table S1). We note that defects within graphenic layers can themselves migrate under the influence of an electron beam.[10] Although such effects can be quantified on pure graphene, they are more difficult to map on heavily doped lattices such as those studied here. It should be borne in mind however that such movements of carbons or dopants within the support layer could also influence the movement of Os atoms, as is apparent in Figure 2a.

It is interesting to consider the possible magnetic states of Os atoms on a graphenic surface. Our DFT calculations on an Os atom on an ideal (without defects or doping) graphene subunit, an aromatic 19-ring $C_{54}H_{18}$ system (Supporting Information Figure S11, Table S2), suggested that this model system is paramagnetic. However, for an infinite graphene lattice, the HOMO−LUMO gap will go to zero, making it unlikely that paramagnetic states will be supported. Experimental magnetic

measurements present a challenge for future work. To further confirm that the doped graphitic surface plays a role in the observed Os migration, we investigated whether the atoms follow Brownian Motion (BM). In BM, each jump is independent and identically distributed according to a normal distribution with variance proportional to the time between observations. We looked for evidence of this in the data, consisting of the migration of five Os atoms on each kind of each surface. First we checked that the size of the jumps in the x and y directions were the same (Supporting Information Figure S12 and Table S3), pooling together all of the jumps for the five separate atoms. There appeared to be no significant difference in the dynamics of migration on the sulfur-doped surface and only a very small difference on the selenium-doped surface. The histograms shown in Figures 3a,b were observed to be similar,
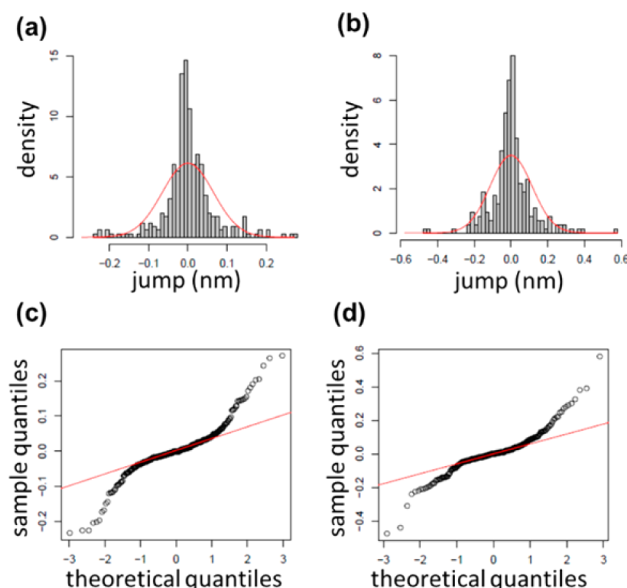

Figure 3. Analysis of the mechanism of hopping of individual Os atoms on the two graphenic surfaces. (a and b) Histograms of pooled jumps of individual Os atoms on B/S and B/Se surfaces, respectively. (c and d) Normal Quantile−Quantile plot of Os atoms hopping on B/S and B/Se surfaces, respectively.

and as such x and y jumps were pooled together for further analysis. We also assumed that the Os atoms were not drifting in any particular direction and so the mean jump would be zero, which also appeared to be confirmed by the data. Next, we fitted a Gaussian density to the pooled jump data and plotted a normal Quantile−Quantile plot to assess deviations from normality (Figures 3c,d).

It is clear from these plots that there are more long-range jumps than would be expected for a Brownian Motion, but for completeness we also performed a Shapiro−Wilk test of normality;[31] both the selenium- and sulfur-pooled data gave p-values below 0.001, and so we can reject the hypothesis that Brownian Motion describes the movement of the Os atoms. Kinetic energy of the e-beam is the main driving force of the dynamic behavior of Os atoms observed in TEM. Returning to the raw data, we see that no large jumps are captured for these two atoms. It is clear from Supporting Information Table S3 that the jump sizes are larger on selenium-doped than on sulfur-doped graphene, but it is nonetheless interesting to investigate whether they come from similar distributions. Supporting Information Figure S13 shows a comparative Quantile−Quantile

plot of their two distributions. Although there is a small amount of deviation from the line in the lower tail, the plot does suggest that the distributions are indeed very similar.

CONCLUSIONS

In conclusion, the new generations of electron microscopes with their atomic resolution capability and ultrafast cameras offer the possibility of imaging dynamic processes in real time. However, there is currently little reported data on such dynamic interactions at the level of the individual atom, owing, in particular, to the fast migration of single atoms on graphene. Here, we have used a new synthetic methodology for the *in situ* formation of graphenic surfaces doped with boron and sulfur (B/S) or selenium (B/Se) heteroatoms. The doping creates anchoring points for individual Os atoms, slowing down their migration so that it is commensurate with the time scale of image capture on an aberration-corrected transmission electron microscope. We have imaged in real time the migration of individual Os atoms and Os_2 dimers on these surfaces. The rate of movement is >20× faster on the B/Se-doped boronic graphenic surface compared to B/S. Indirectly, through choice of the dopants, our methodology can provide control of atomic dynamics and might lead to a wide range of potential applications (*e.g.*, patterning on surfaces, security labeling at the atomic level, sealing confidential documents). There is much scope for extending the fabrication to a wider range of doped-graphenic matrices, so as to further modify the surface dopants and the metal atom migration rates, and to the deposition of other metal atoms (*e.g.*, other precious metals such as Au, Pt, and Pd).

ASSOCIATED CONTENT

Ⓢ Supporting Information

HRTEM images of Os atoms on B/S surface and FFT analysis (Figure S1), EELS and EDX analysis of B/S and B/Se surfaces (Figure S2), Os atom migration on B/S (video Figure S3, with superimposition on hexagonal grid in video Figure S5) and B/Se (video Figure S4, with superimposition on hexagonal grid in video Figure S6) surfaces, analysis of trajectory of Os on B/S surface and trapping sites (Figure S7), Os speed and Os—Os bond lengths (Table S1), comparative movement of Os on B/S and B/Se surfaces (video Figure S8), migration of Os_2 on B/Se (video Figure S9) and B/S (video Figure S10) surfaces, DFT geometry optimizations of Os on a graphene subunit (Figure S11, parameters in Table S2), histograms of Os jump sizes on B/S and B/Se surfaces (Figure S12, standard deviations and corrected median absolute deviations for the moves of Os atoms in Table S3), and normal Quantile—Quantile plots (Figure S13). The Supporting Information is available free of charge on the ACS Publications website at DOI: 10.1021/acs.chemmater.5b01853.

AUTHOR INFORMATION

Corresponding Authors
*(N.P.E.B.) E-mail: n.barry@warwick.ac.uk.
*(P.J.S.) E-mail: p.j.sadler@warwick.ac.uk.

Notes
The authors declare no competing financial interest.

ACKNOWLEDGMENTS

REFERENCES

(1) Isaacson, M.; Kopf, D.; Utlaut, M.; Parker, N. W.; Crewe, A. V. Direct observations of atomic diffusion by scanning transmission electron microscopy. *Proc. Natl. Acad. Sci. U.S.A.* **1977**, *74*, 1802−1806.

(2) Utlaut, M. Direct observation of the behavior of heavy single atoms on amorphous carbon substrates. *Phys. Rev. B* **1980**, *22*, 4650−4660.

(3) Lebedeva, M. A.; Chamberlain, T. W.; Schröder, M.; Khlobystov, A. N. New Pathway for Heterogenization of Molecular Catalysts by Non-covalent Interactions with Carbon Nanoreactors. *Chem. Mater.* **2014**, *26*, 6461−6466.

(4) Rodríguez-Zamora, P.; Yin, F.; Palmer, R. E. Enhanced Immobilization of Gold Nanoclusters on Graphite. *J. Phys. Chem. A* **2014**, *118*, 8182−8187.

(5) He, Z.; He, K.; Robertson, A. W.; Kirkland, A. I.; Kim, D.; Ihm, J.; Yoon, E.; Lee, G.-D.; Warner, J. H. Atomic Structure and Dynamics of Metal Dopant Pairs in Graphene. *Nano Lett.* **2014**, *14*, 3766−3772.

(6) Ibáñez, M.; Cabot, A. All Change for Nanocrystals. *Science* **2013**, *340*, 935−936.

(7) Egerton, R. F. Beam-Induced Motion of Adatoms in the Transmission Electron Microscope. *Microsc. Microanal.* **2013**, *19*, 479−486.

(8) Hardcastle, T. P.; Seabourne, C. R.; Zan, R.; Brydson, R. M. D.; Bangert, U.; Ramasse, Q. M.; Novoselov, K. S.; Scott, A. J. Mobile metal adatoms on single layer, bilayer, and trilayer graphene: An ab initio DFT study with van der Waals corrections correlated with electron microscopy data. *Phys. Rev. B* **2013**, *87*, 195430.

(9) Lee, J.; Zhou, W.; Pennycook, S. J.; Idrobo, J.-C.; Pantelides, S. T. Direct visualization of reversible dynamics in a Si6 cluster embedded in a graphene pore. *Nat. Commun.* **2013**, *4*, 1650.

(10) Zoberbier, T.; Chamberlain, T. W.; Biskupek, J.; Kuganathan, N.; Eyhusen, S.; Bichoutskaia, E.; Kaiser, U.; Khlobystov, A. N. Interactions and Reactions of Transition Metal Clusters with the Interior of Single-Walled Carbon Nanotubes Imaged at the Atomic Scale. *J. Am. Chem. Soc.* **2012**, *134*, 3073−3079.

(11) Kotakoski, J.; Mangler, C.; Meyer, J. C. Imaging atomic-level random walk of a point defect in graphene. *Nat. Commun.* **2014**, *5*, 4991.

(12) Rodríguez-Manzo, J. A.; Cretu, O.; Banhart, F. Trapping of Metal Atoms in Vacancies of Carbon Nanotubes and Graphene. *ACS Nano* **2010**, *4*, 3422−3428.

(13) Cretu, O.; Krasheninnikov, A. V.; Rodríguez-Manzo, J. A.; Sun, L.; Nieminen, R. M.; Banhart, F. Migration and Localization of Metal Atoms on Strained Graphene. *Phys. Rev. Lett.* **2010**, *105*, 196102.

(14) Gong, C.; Robertson, A. W.; He, K.; Ford, C.; Watt, A. A. R.; Warner, J. H. Interactions of Pb and Te atoms with graphene. *Dalton Trans.* **2014**, *43*, 7442−7448.

(15) Muhich, C. L.; Westcott, J. Y.; Morris, T. C.; Weimer, A. W.; Musgrave, C. B. The Effect of N and B Doping on Graphene and the Adsorption and Migration Behavior of Pt Atoms. *J. Phys. Chem. C* **2013**, *117*, 10523−10535.

(16) Zhang, T.; Zhu, L.; Yuan, S.; Wang, J. Structural and Magnetic Properties of 3d Transition-Metal-Atom Adsorption on Perfect and Defective Graphene: A Density Functional Theory Study. *ChemPhysChem* **2013**, *14*, 3483−3488.

(17) Lazar, P.; Zhang, S.; Šafářová, K.; Li, Q.; Froning, J. P.; Granatier, J.; Hobza, P.; Zbořil, R.; Besenbacher, F.; Dong, M.; Otyepka, M. Quantification of the Interaction Forces between Metals and Graphene by Quantum Chemical Calculations and Dynamic Force Measurements under Ambient Conditions. *ACS Nano* **2013**, *7*, 1646−1651.

(18) Zhang, W.; Sun, L.; Xu, Z.; Krasheninnikov, A. V.; Huai, P.; Zhu, Z.; Banhart, F. Migration of gold atoms in graphene ribbons: Role of the edges. *Phys. Rev. B* **2010**, *81*, 125425.

(19) Nakada, K.; Ishii, A. Migration of adatom adsorption on graphene using DFT calculation. *Solid State Commun.* **2011**, *151*, 13−16.

(20) Herberhold, M.; Yan, H.; Milius, W. The 16-electron dithiolene complexes (p-cymene)M[S2C2(B10H10)] (M=Ru, Os) containing both η6-(p-cymene) and η2-(ortho-carborane-dithiolate): adduct

formation with Lewis bases, and X-ray crystal structures of (p-cymene)Ru[S2C2(B10H10)](L) (L=PPh3) and {(p-cymene)Ru-[S2C2(B10H10)]}2(μ-LL) (LL=Ph2PCH2CH2PPh2 and N2H4). *J. Organomet. Chem.* **2000**, *598*, 142−149.

(21) Thevenaz, P.; Ruttimann, U. E.; Unser, M. A pyramid approach to subpixel registration based on intensity. *Image Process., IEEE Trans.* **1998**, *7*, 27−41.

(22) Neese, F. The ORCA program system. *Wiley Interdiscip. Rev.: Comput. Mol. Sci.* **2012**, *2*, 73−78.

(23) Schaefer, A.; Horn, H.; Ahlrichs, R. Ahlrichs def2 basis sets. *J. Chem. Phys.* **1992**, *97*, 2571.

(24) Andrae, D.; Häußermann, U.; Dolg, M.; Stoll, H.; Preuß, H. Energy-adjustedab initio pseudopotentials for the second and third row transition elements. *Theor. Chim. Acta* **1990**, *77*, 123−141.

(25) Weigend, F.; Ahlrichs, R. Balanced basis sets of split valence, triple zeta valence and quadruple zeta valence quality for H to Rn: Design and assessment of accuracy. *Phys. Chem. Chem. Phys.* **2005**, *7*, 3297−3305.

(26) Perdew, J. P.; Burke, K. Generalized Gradient Approximation Made Simple. *Phys. Rev. Lett.* **1996**, *77*, 3865−3868.

(27) Goerigk, L.; Kruse, H.; Grimme, S. Benchmarking Density Functional Methods against the S66 and S66x8 Datasets for Non-Covalent Interactions. *ChemPhysChem* **2011**, *12*, 3421−3433.

(28) Barry, N. P. E.; Pitto-Barry, A.; Sanchez, A. M.; Dove, A. P.; Procter, R. J.; Soldevila-Barreda, J. J.; Kirby, N.; Hands-Portman, I.; Smith, C. J.; O'Reilly, R. K.; Beanland, R.; Sadler, P. J. Fabrication of crystals from single metal atoms. *Nat. Commun.* **2014**, *5*, 3851.

(29) Schindelin, J.; Arganda-Carreras, I.; Frise, E. Fiji: an open-source platform for biological-image analysis. *Nat. Methods* **2012**, *9*, 676−682.

(30) Arblaster, J. W. Densities of Osmium and Iridium. *Platinum Metals Rev.* **1989**, *33*, 14−16.

(31) Shapiro, S. S.; Wilk, M. B. An analysis of variance test for normality (complete samples). *Biometrika* **1965**, *34*, 591611.